



# Voltage-controlled of photocurrent in silicon planar metal-semiconductor-metal structures

S.Khunkhao<sup>a</sup>, P. Liengpradis<sup>a</sup>, W.Chankaipol<sup>a</sup>, S.Niemcharoen<sup>b</sup>, A.Ruangphanit<sup>c</sup>,  
N.Phongphanthra<sup>c</sup>, Kazunori SATO<sup>d</sup>

<sup>a</sup> Department of Electrical Engineering, Faculty of Engineering, Sripatum University,  
61 Phahonyothin Road, Saenanihkom, Jatujak, Bangkok, 10900 Thailand.  
Email: sanya.kh@spu.ac.th

<sup>b</sup> Electronics Research Center, Faculty of Engineering, King Mongkut's Institute of Technology  
Ladkrabang, Bangkok, Thailand Email: knsurasa@kmitl.ac.th

<sup>c</sup> Thai Microelectronics Center (TMEC), National Electronics and Computer Technology (NECTEC)  
51/4 Moo 1, Wangtakiean, Muang Chachoengsao, Chachoengsao24000, Thailand.

<sup>d</sup> Department of Electronics, School of Information Technology and Electronics, Tokai University,  
Kitakaname 1117, Hiratsuka, Kanagawa, 259-1292 Japan. Email:kznrsato@keyaki.cc.u-tokai.ac.jp

## Abstract

The bias-controllable photocurrent characteristic by using planar MSM structures with both depleted and undepleted regions under dc and ac optical illumination condition has been proposed at the active area. The structure has two co-planar Mo/n-Si Schottky-barrier junctions on silicon of resistivity 9-12  $\Omega$ -cm and the electrode separation is 20  $\mu$ m. By introducing an undepleted region between Schottky barriers on both sides, the depleted region width at the front surface under illumination varies with bias applied, where this region would be more sensitive to optical quantity than the undepleted region to generate the photocurrent. Therefore, this structure is expected to show the output photocurrent as the function of not only optical illumination intensity but applied bias due to laterally spreading of space-charge-region (SCR). Making use of planar molybdenum n-type silicon molybdenum (Mo/n-Si/Mo) structures, it has been experimentally demonstrated that such a structure exhibits voltage-controllability of photocurrents whilst maintaining the inherent function converting optical signal into electronic signal. An appreciable improvement in obtaining output photocurrent was confirmed from both dc and low frequency 100Hz-100 kHz photoresponse properties. It was found that this structure shown an appreciable voltage controllability of the photocurrent of this structure.

**Keywords:** Planar metal-semiconductor-metal structure; Optical sensor; Space-charge-region.

## 1. Introduction

A planar metal-semiconductor-metal (MSM) structure is simply composed of two back-to-back or face-to-face Schottky barriers placed flatwise and it has some advantages as a viable photosensing structure. One of them is the feasibility of fabricating optoelectronic integrated circuits (OEICs). Because of its simple and compatible fabrication process such

as forming Schottky barrier of MSM structure, the process is essentially identical to the gate metallization of field effect transistors (FETs). Moreover, although there may be design trade-offs for optimizing between speed and efficiency, such a structure could have lower capacitance and be often transit-time-limited to meet wide band operation. In this study, Si-based planar MSM photosensing structures were





treated with dc and ac optical response at low frequencies 100Hz-100 kHz modulated optical illumination.

## 2. Experimental

### 2.1 Sample Preparation

The test samples have planar molybdenum/n-type silicon/molybdenum (Mo/n-Si/Mo) structure prepared by following process. This structure has Schottky barrier junction between evaporated molybdenum and n-type silicon. Electron-beam evaporation of molybdenum was carried out onto an n-type mirror polished surface of silicon of resistivity (9-12) $\Omega$ cm, which had been cleaned chemically and then rinsed by deionized (DI) water in ultrasonic bath beforehand.

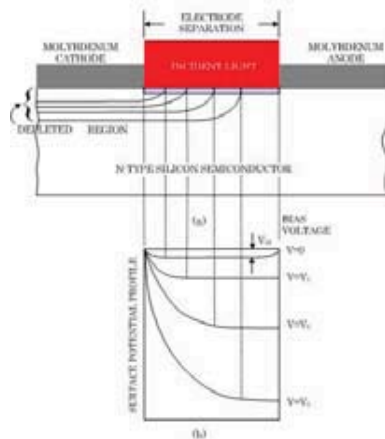


Fig. 1. Schematic illustration of cross-sectional view of the test device with depletion layer (a) and potential profiles under various bias voltages (b). In the potential profiles, Schottky effect at cathode edge and depletion layer of anode forward-biased are ignored.

The thickness of deposited molybdenum film was approximately 3000Å. Molybdenum film so formed works as Schottky barrier metal and electrodes as well. Figure 1 (a) illustrates the cross-sectional configuration of the sample, which was completed using photolithographic lift-off technique. The configuration is symmetrical and the size of two electrodes is the same and of 3mm $\times$ 3mm. Thus, the structure is face-to-face structure of two Schottky junctions. The sample is not interdigitated but of single slit type. The internal separation between the electrodes is 20  $\mu$ m, which is wide enough for the depleted region of both junctions not to get

touch with one another even when bias voltage is applied. Under a bias, the anode is forward-biased and the cathode is reversed-biased. Thus, the band diagram of the structure under a bias much larger than its built-in voltage is assumed a single junction. From the forward current-voltage (I-V) characteristics and capacitance-voltage (C-V) characteristics under dark of independent Schottky-barriers, the barrier height and built-in voltage were estimated to lie around 0.70 eV and 0.23 eV, respectively [1]. The scanning electron microscope (SEM) image of the experimental samples used in this study is shown in Fig. 2.

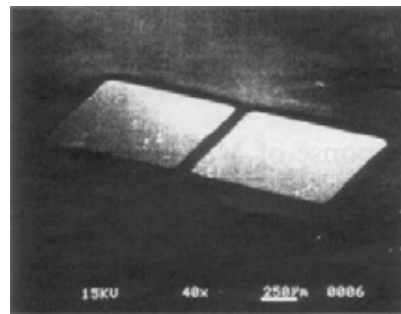


Fig. 2. SEM image of a sample with 100  $\mu$ m electrode separation (before bonding)

### 2.2 MEASUREMENT PROCEDURE

The current versus applied bias (I-V) characteristics were measured under optical illumination and in the dark conditions. The block diagram of the set up for measurements of I-V characteristics is shown in Fig. 3. All measurements were carried out in the temperatures (295–300) $^{\circ}$ C. The increase in the dark current with applying bias might be attributed to the charge generation in the expanding SCR under reverse bias [2] and/or the incompleteness of fabrication process of the samples.

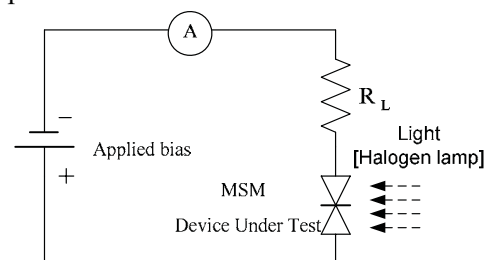


Fig 3. Current-voltage I-V characteristic measurement system.





### 3. Results and Discussions

#### 3.1 Static DC characteristics

Figure 4 shows the typical photocurrent versus relations at room temperature under different illumination levels from a halogen lamp. Here the photocurrent component was obtained by subtracting the current under dark from the device current at each corresponding bias voltage. Each plot seems to be divided into two regions: the gradually increasing and rapidly increasing regions with bias. Since the present sample has the electrodes widely separated to avoid electronic interference between two junctions, the lateral separated in the depleted region would be more efficient to generated the photocurrent than the residual undepleted neutral region.

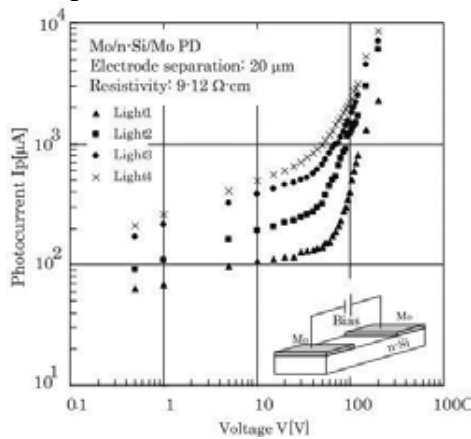


Fig 4. Photocurrent-voltage characteristics of a Mo/n-Si/Mo structure having 20μm electrode separation.

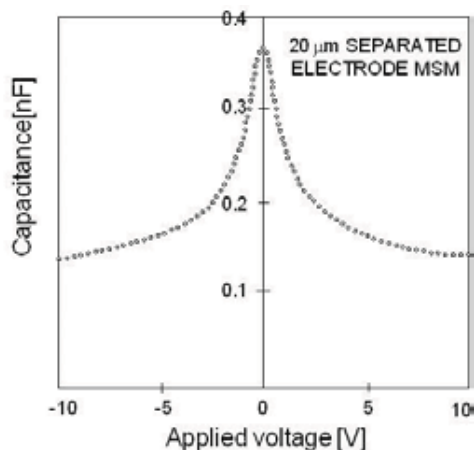


Fig.5. C-V characteristic of the sample appeared in Fig.4.

This would be the reason why the total photocurrent shows gradual increase with bias. The other region showing rapid increase in the photocurrent above about 12V seems to be under the onset of avalanche breakdown of the Schottky-junction reverse-biased, where the junction on the other side is, of course, forward-biased and its band structure is almost flattened. Under illuminated conditions, however, its saturation character seems to be worse than in the dark. The reason for this is discussed below in detail. Figure 5 shows the capacitance-voltage (C-V) characteristics of sample as in Fig. 4. Its voltage dependence is rather smaller than the ideal one treated by Sze et al. [3]. These results imply that the measured characteristic involves the contribution from the stray capacitance of the measurement unit.

When a bias voltage is applied between the electrodes, one Schottky-junction is reverse-biased and the other junction is forward-biased. Such a structure is expected to show lateral spreading of its space-charge-region (SCR) at the Schottky-barrier reverse-biased, the spreading of which is possible to be controlled by bias voltage (V). According to the simplified model of such a structure, the width of the lateral spreading  $W(V)$  of the SCR of the Schottky-junction reverse-biased in the direction of profiling is expressed semi-empirically as [4].

$$W(V) = \sqrt{\beta(V_{bi} + V)} \quad (1)$$

with,  $\beta = 2\epsilon_s/qN_D = 16.5\mu\text{m}^2/\text{V}$  and  $V_{bi}$  : built-in voltage. A single Schottky-barrier prepared in the same process furnishing a back contact has shown the built-in potential of about 0.23 eV. Therefore, the bias dependence of the SCR width expressed as Eq. (1) is expected to be as shown in Fig. 4 before breakdown bias applied. It is found that, as far as the bias dependence of the plots of the experimental photocurrents concerns, quite similar dependence has been obtained except lower bias regions. In the experimental plots, however, a value bias-independent seems to add to Eq. (1) for each plot. Considering the optical illumination incident onto the whole region between both electrodes, this value is to be the contribution from the diffusion of carriers. Correspondingly, the following experimental (semi-empirical)





expression denoting the photocurrent  $I_p$  is proposed,

$$I_p = \eta[\alpha W(V) + L] = \eta[\alpha\sqrt{\beta(V+V_{bi})} + L] \quad (2)$$

Here  $\eta$  and  $\alpha$  are the fitting parameters which can be determined experimentally. The factor  $\eta$  includes the contributions of the size of the active area, the intensity of incident light, and also quantum efficiency. Another parameter  $\alpha$  is the effectiveness ratio of the photocurrent generated in the SCR to the current due to the carriers generated in the undepleted region [5,6].  $L$  is the diffusion length of carriers photoexcited in the undepleted region. As far as Eq.(2) is employed, for a certain sample, the ratio of the value  $\alpha\sqrt{\beta}$  to  $L$  would be essentially constant.

Another support to the present explanation is the photocurrent behavior observed in the samples made using different resistivity wafers of (9-12) $\Omega\text{cm}$ , 23 $\Omega\text{cm}$  (40-50) $\Omega\text{cm}$  which have 2000 $\mu\text{m}$  electrode separation. Figure 6 shows  $I_p$ - $V$  characteristics under certain illumination intensity in log-log scale after the contribution of the bias-independent term is excluded. One finds that at higher voltages each plot has the same slope of 0.5, suggesting that the current follows the spreading of the SCR given by Eq.(1). The solid line in the figure denotes the line with the slope of 0.5 to guide the eye. The physical parameters used for calculations are given in Table 1.

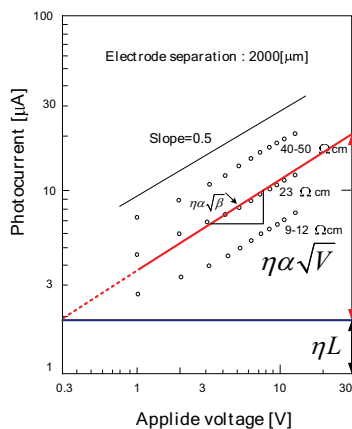


Fig.6.  $I_p$  -  $V$  characteristics in log-log scale for the samples made on wafers of three different resistivities, (9-12), 23 and (40-50) $\Omega\text{cm}$ , which have the same electrode separation of 2000 $\mu\text{m}$ .

According to the above consideration, the SCR must be much more efficient in generating photocurrents than the residual undepleted neutral region. To confirm this directly, the photocurrent measurements were performed by moving the irradiating position of the focused beam a He-Ne laser. Figure 7 illustrates the photocurrent distribution profile versus the irradiating position for a 2000 $\mu\text{m}$  electrode separated sample, which was obtained by moving the beam at every 15  $\mu\text{m}$ -step. From this figure, it is apparent that the side of the Schottky barrier reverse-biased can generate appreciable photocurrent. Therefore, it can be mentioned that the SCR is quite efficient in generating photocurrents comparing to the residual undepleted region.

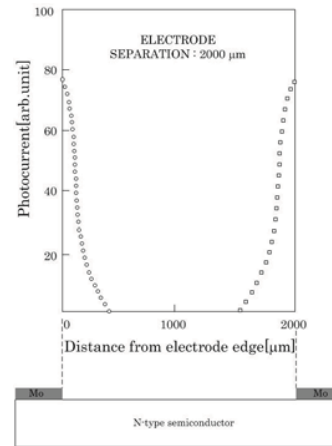


Fig. 7. Open circles are for photocurrent profile at the edge of the electrode reverse-biased on the left-hand side. When the sign of bias is reversed, the profile given by open squares is observed. Electrode separation is 2000  $\mu\text{m}$ .

**Table1:** List of symbols and their value used in numerical calculation and in the text

Symbol	Value
$V$ : applied bias	1-20V
$V_{bi}$ : built-in voltage of the Mo/n-Si	0.23 eV
$W(V)$ : depletion region width	$\sqrt{[\beta(V_{bi} + V)]}$
$\beta = 2\epsilon_s / qN_D$	16.5 $\mu\text{m}^2/\text{V}$
$\epsilon_s$ : permittivity of semiconductor	$1.054 \times 10^{-10}$ F/m
$q$ : elementary charge	$1.60 \times 10^{-19}$ C
$N_D$ : donor concentration	$8 \times 10^{13} \text{cm}^{-3}$
$L$ : diffusion length of minority carriers	70 $\mu\text{m}$
$k$ : Effectiveness ratio to undepleted region	2.6







### 3.2 Signal (ac) characteristics

This section will treat the low frequency optical signal response of the planar MSM structures proposed. The purpose of this section is to present the influence of operating condition on the low frequency (1kHz-1MHz) photoelectric response of planar Mo/n-Si/Mo structure with long neutral region. Optical response was measured using sinusoidally modulated He-Ne laser signal via an acousto-optic modulator (AOM). Figure 8 shows the block diagram for measurements of ac characteristics. An ND filter was used to control the light intensity and thus the photocurrent of the device. The signal to be detected was fed to a load of 2 k $\Omega$  connected in series with the device under test.

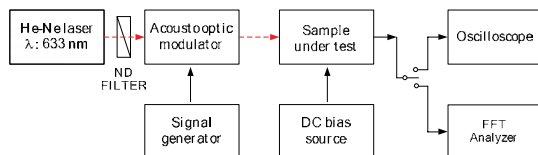


Fig. 8. Schematic diagram of the setup for photoresponse measurements.

Then, the voltage drop across the load was conducted to an oscilloscope to observe instantaneous demodulated signals or to a Fast Fourier Transform (FFT) spectrum analyzer to view the signals received in frequency domain.

Figure 9 is the typical photoresponse vs. frequency plots for a 2000  $\mu\text{m}$  separated electrode sample under a bias of 20V, taking the load as a parameter changing from 500 $\Omega$  to 20k $\Omega$ , respectively. The plots are normalized at low frequency region where the spectra are frequency-independent. It can be seen that the plot at smaller load (500  $\Omega$ ) possesses two different turn-over frequencies. These results imply that the lower turn-over frequency is due to intrinsic nature of this device. Since the current from the neutral region is due to diffusion process, its turn-over frequency is low (around 30 kHz). Turn-over frequency, here, means the frequency at which the response starts its decreasing. The higher turn-over frequency (around 70 kHz) must be due to drift process. The higher turn-over frequency is limited by the resultant time-constant including the load resistance, and thus due to extrinsic operating conditions [7].

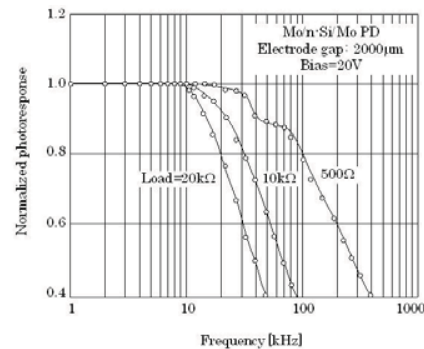


Fig. 9. Normalized photoresponse versus frequency of a 2000 $\mu\text{m}$  separated electrode sample with various loads.

One expects in low frequency response the behavior similar to dc response as far as the diffusion current component responds. Measurements of optical response were carried out for the sample as examined in dc scheme and shown in Fig.4. Figures 10(a) and (b) show the typical oscilloscope traces of the signal (frequency: 10 kHz) detected at two biases, 1V and 20V, respectively. In Figure 10, the amplitude of the demodulated waveform increases from 2.8mV (peak-to-peak) at a bias  $V=1\text{V}$  to 6.8mV at  $V=20\text{V}$  apparently showing the bias controlled iris effect is occurring.

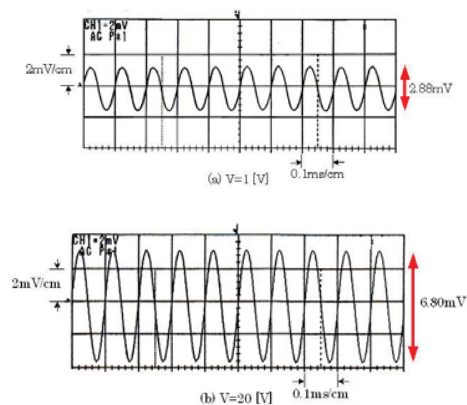
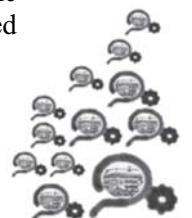


Fig. 10. Oscilloscope traces of the demodulated signal waveforms at 10 kHz in time domain by a three-finger MSM-PD structure at biases  $V = 1\text{V}$  (a) and  $20\text{V}$  (b) .

One finds that essentially the same waveform has been obtained and demodulated [10-13]. Although the relation between the voltages applied to the device and the expected output current is nonlinear due to Eq. (1), the relation between the optical signal to be detected





and the detected electronic signal would be linear because the output current is proportional to the intensity of the optical signal to be detected [8]. In order to check the spurious effect in the demodulation process, the frequency distribution of the original waveform and the demodulated waveform were observed using an FFT spectrum analyzer as shown in Fig. 11.

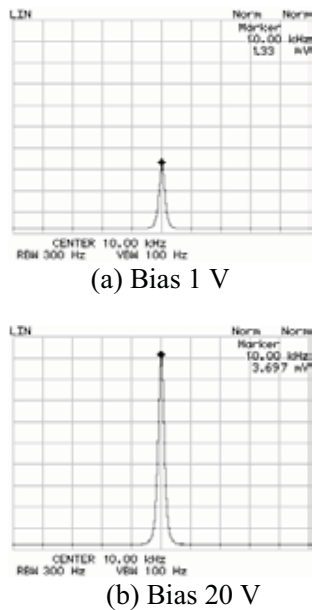


Fig.11. Spectra of the demodulated signals at biases  $V=1V$ (a) and  $20V$ (b) at 10 kHz for the same device as appeared in Fig.10 in frequency domain by an FFT spectrum analyzer.

#### 4. Conclusion

Bias-controllable photocurrent characteristics using planar Mo/n-Si/Mo systems with depleted and undepleted region at the active area were examined and confirmed experimentally. It can be concluded that one can control the photocurrent in a planar MSM structure under dc optical illumination by varying bias. As it were, one can give these structures an electronic iris effect by introducing an undepleted neutral region between electrodes, maintaining the function of changing the optical signal into electronic signal. The neutral region as well as the depleted region plays a key role for this effect. Then, their optoelectronic response at low frequency range (1kHz to 1MHz) has been examined. It was observed that the spectra of the photoresponse consist of the contributions of both the depleted and undepleted neutral

regions. At the same time, the function of an electronic iris controlled by the applied bias was confirmed without introducing spurious effect.

#### 5. Acknowledgement

The authors are thankful to Assoc.Dr.W. Titiroongruang of King Mongkut's Institute of Technology Ladkrabang for many helpful discussions. Continuous encouragement of Dr.R.P.Phukkamarn of Sripatum University is deeply appreciated. This work was supported in part by The Thailand Research Fund under and Commission Higher Education Grant No. MRG5080004.

#### 6. References

- [1] S.M Sze, "Physics of Semiconductor Devices, 2<sup>nd</sup> ed. John-Wiely, New York, 1981
- [2] Snowden CM. Semiconductor device modeling, London, Peter Peregrinus,1988.
- [3] Niemcharoen S, Kobayashi K, Kimura M, Sato K. Voltage dependence of photocurrent in metal-semiconductor-metal structures under front-illuminated conditions. Solid-State Electron 2000; 44: 2161.
- [4] Grove As, Physics and technology of semiconductor devices. New York: John Wiley, 1967.
- [5] C. S. Harder, B. J. Van Zeghbroeck, M. P. Kesler, H. P. Meier, P. Vettiger, D. J. Webb, P. Wolf "High-speed GaAs/AlGaAs optoelectronic devices for computer applications", IBM J.Res.Develop, High-speed semiconductor devices, Vol.34, 1990, pp. 568-584
- [6] H. Melchior and W.T. Lynch, "Signal and Noise Response of High Speed Germanium Avalanche Photodiodes," IEEE. Trans. Electron Devices, vol. ED-13, Dec. 1966, pp. 829-838..
- [7] A. Goetzberger, B. McDonald, R. H. Haitz, and R. M. Scarlett "Avalanche Effects in Silicon p-n Junctions. II. Structurally Perfect Junctions", J. Appl. Phys. **34**, 1963, pp. 1581
- [8] T. Masui, S. Khunkhao, K. Kobayashi, S. Niemcharoen, S. Supadech, K. Sato, "Photosensing properties of interdigitated metal semiconductor-metal structures with undepleted region," Solid-State Electron. Vol.43, pp.1811,2003.

